Physica B 179 (1992) 6–18
North-Holland

PHYSICA B

Frequency dependent biaxial anisotropy due to the Rosenfeld tensor, an FMD computer simulation

M.W. Evans[1] and S. Woźniak[2]

Institute of Physical Chemistry, University of Zurich, Winterthurerstrasse 190, CH-8057 Zurich, Switzerland

Received 11 September 1991
Revised manuscript received 18 November 1991

A novel biaxial anisotropy (BA), accompanied by torque frequency doubling, is reported from a field applied molecular dynamics (FMD) computer simulation of (S)-CHBrClF in a right and left circularly polarised pump laser. The BA is observed as anisotropy in several time correlation functions computed in the presence of the laser, and is measurable experimentally as a refractive index difference between circularly polarised and incoherently or linearly polarised probe laser radiation.

1. Introduction

In a series of papers [1–6] we have developed the technique of field applied molecular dynamics (FMD) computer simulation for a number of non-linear optical phenomena: (a) static and dynamic electric polarisation due to the non-linear conjugate product ($\Pi_{ij}^{(A)}$) [1] of an intense, circularly polarised, laser, (b) the optical Kerr effect [2], (c) the inverse Faraday effect and inverse magnetochiral birefringence [3], (d) optical NMR [4], (e) circular dichroism and optical rotatory dispersion [5], and (f) the frequency doubled optical Stark effect [6]. In all cases the forces loop of a standard molecular dynamics computer simulation algorithm TETRA was modified to take an extra, external, torque due to each non-linear optical effect (a) to (f), and a range of novel information extracted [1–6] on the effect of the laser on the molecular ensemble.

In this paper the FMD technique is used to reveal a novel bi-axial anisotropy [5] due to the Rosenfeld tensor which is accompanied by torque frequency doubling (BAFD). Bi-axial anisotropy indicates bi-axial birefringence (BBFD), which must be distinguished at the outset from circular birefringence. In the former, the refractive index is different in the propagation axis of the laser (Z) and orthogonal (X and Y) directions. Circular birefringence is the refractive index difference measured with right and left circularly polarised electromagnetic radiation. Bi-axial birefringence was shown in ref. [5] to accompany circular birefringence in chiral ensembles, and to exist in some achiral point groups through the mediacy of off-diagonal elements of the Rosenfeld tensor. Bi-axial birefringence of the type reported in ref. [5] is the *same* for right and left circularly polarised radiation, but vanishes when it is incoherently or linearly polarised [5]. Therefore there exists a difference in the refractive index of water, for example, when measured in the same propagation axis, Z, with firstly a circularly polarised laser, and secondly an unpolarised laser. This difference gives unique information [5] on the Rosenfeld (i.e. electric dipole/magnetic dipole) tensor in achiral molecules.

[1] Permanent address: 433 Theory Center, Cornell University, Ithaca, NY 14853, USA.
[2] Permanent address: Nonlinear Optics Division, Institute of Physics, Adam Mickiewicz University, Grunwaldzka 6, 60-780 Poznań, Poland.

In section 2 of this paper the torque responsible for BBFD is described in a frame of reference fixed by the principal molecular moments of inertia of (S)-CHBrClF, and whose magnetic and electric origins are described in detail. In section 3 the FMD methods are summarised briefly; section 4 presents evidence from FMD for the existence of BBFD using the anisotropy of various time correlation functions computed in the presence of the BBFD torque. In this section it is shown that BBFD is not accompanied by circular birefringence, and frequency doubling consequently isolates bi-axial birefringence from circular birefringence due to the same Rosenfeld tensor elements. Finally, a discussion is given of the experimental methods likely to be used for the first measurement of BBFD.

2. Description of the torque

The technique of FMD codes into forces loop of a standard molecular dynamics algorithm (of any suitable variety) an extra torque set up between the external field and each molecule of the ensemble. There is, furthermore, no restriction on the type of field which can be used, provided it forms a torque with the individual molecules (or atoms). The integral over configuration of the torque is related to the work done by the interaction of field and molecule, which is equal in magnitude but opposite in sign to the interaction potential energy [7]. The latter is a term in the Hamiltonian describing the interaction process, and this reveals why the torque method is a rigorous and general description which is approximated numerically by FMD.

References [1–6] contained a detailed description of some of the relevant torques in non-linear optics, where an intense pump laser interacts with a molecular dynamical ensemble. In FMD this interaction is treated classically, using the equations of the electromagnetic plane wave, but in general there is no reason why the method cannot be extended, for example, to the quantum mechanics of, and chaotic phenomena in, non-linear optics [8, 9]. The data banks accompanying refs. [1–6], and animation videos [10, 11] provide evidence of the information provided by FMD analysis of non-linear optics. In this paper we shall be concerned primarily with orientational rise transients which occur immediately after the application of the laser (switching on the torque) and time correlation functions [1–6, 12] in the presence of the laser. (In real experiments [13, 14] this would be a pump laser pulse, for example, or as in ref. [5] the probe laser or broad band radiation of an instrument designed to measure optical rotatory dispersion and circular dichroism in the far infrared [15, 16]. In bi-axial birefringence [5] the field is simply a probe electromagnetic wave with given polarisation characteristics.) For BBFD, consider an electromagnetic plane wave propagating in the Z axis of the laboratory frame (X, Y, Z) through an ensemble [5] of (S)-CHBrClF molecules, enantiomers of C_1 molecular point group symmetry. It is well known that the electric field (E_j) of the plane wave induces [5] a magnetic dipole moment $(m_i^{(\mathrm{ind})})$ in the molecule through the intermediacy of the complex Rosenfeld tensor $({}^{m}\alpha_{ij}^{e})$ of semi-classical theory [17]. Similarly, the magnetic field (B_j) of the plane wave induces an electric dipole moment $(\mu_i^{(\mathrm{ind})})$ through different components of the Rosenfeld tensor $({}^{e}\alpha_{ij}^{m})$. Accordingly, the torque to be considered in the frame $(1, 2, 3)$ of the principal molecular moments of inertia of (S)-CHBrClF is

$$\begin{aligned} \boldsymbol{T} &= \boldsymbol{T}^{(1)} + \boldsymbol{T}^{(2)} , \\ \boldsymbol{T}^{(1)} &= -\boldsymbol{\mu}^{(\mathrm{ind})} \times \boldsymbol{E} , \\ \boldsymbol{T}^{(2)} &= -\boldsymbol{m}^{(\mathrm{ind})} \times \boldsymbol{B} , \end{aligned} \tag{1}$$

where we have used vector notation. In order to work out the scalar elements of the torque it is useful to convert to subscript tensor notation [17] using the Einstein convention of summation over repeated indices. In this notation the same torque becomes

$$
\begin{aligned}
T_l &= T_l^{(1)} + T_l^{(2)} , \\
T_l^{(1)} &= -\epsilon_{lij}\, {}^{e}\alpha_{ik}^{m} B_k E_j , \\
T_l^{(2)} &= -\epsilon_{lij}\, {}^{m}\alpha_{ik}^{e} E_k B_j ,
\end{aligned}
\tag{2}
$$

where ϵ_{lij} is the rank three totally antisymmetric unit tensor (or Levi–Civita symbol).

The tensors ${}^{e}\alpha_{ij}^{m}$ and ${}^{m}\alpha_{ij}^{e}$ can be written [5, 18] as

$$
\begin{aligned}
{}^{e}\alpha_{ij}^{m} &= {}^{e}\hat{\beta}_{ij}^{m} + \mathrm{i}\, {}^{e}\hat{\gamma}_{ij}^{m} , \\
{}^{m}\alpha_{ij}^{e} &= {}^{m}\hat{\beta}_{ij}^{e} + \mathrm{i}\, {}^{m}\hat{\gamma}_{ij}^{e} .
\end{aligned}
\tag{3}
$$

In the vicinity of optical resonance each part becomes complex [17, 18]:

$$
\begin{aligned}
{}^{m}\hat{\gamma}_{ij}^{e} &= {}^{m}\gamma_{ij}^{e} + \mathrm{i}\, {}^{m}\gamma_{ij}^{e'} , \\
{}^{m}\hat{\beta}_{ij}^{e} &= {}^{m}\beta_{ij}^{e} + \mathrm{i}\, {}^{m}\beta_{ij}^{e'} .
\end{aligned}
\tag{4}
$$

Clearly, several torques can be formed from the various parts of the Rosenfeld tensor. We narrow consideration for BBFD to the gamma tensors ${}^{m}\hat{\gamma}_{ij}^{e}$ and ${}^{e}\hat{\gamma}_{ij}^{m}$.

The real part of each of these, ${}^{m}\gamma^{e}$ and ${}^{e}\gamma^{m}$, are known as the polarisability tensors of optical rotatory dispersion ("ORD tensors") and the imaginary parts ${}^{m}\gamma^{e'}$ and ${}^{e}\gamma^{m'}$ are the polarisability tensors of circular dichroism ("CD tensors"). It was shown in ref. [5] that the ORD tensors mediate bi-axial birefringence in chiral and achiral ensembles of appropriate molecular point group symmetry, such as the C_{2v} symmetry of the water molecule.

The torque used in ref. [5],

$$
\boldsymbol{T} = -\boldsymbol{\mu}^{(\mathrm{ind})} \times \boldsymbol{E}^{*} - \boldsymbol{m}^{(\mathrm{ind})} \times \boldsymbol{B}^{*} ,
\tag{5}
$$

removes the phase of the plane wave by using multiplication of complex conjugates, E_i^{*}, for example, denoting the complex conjugate of E_i. However, in the torques (1) or (2) of this paper a key difference is that frequency doubling occurs through products such as $B_k E_j$ of electric and magnetic components

$$
\begin{aligned}
\boldsymbol{E}^{(\mathrm{L})} &= E_0(\boldsymbol{e}_X + \mathrm{i}\boldsymbol{e}_Y)\exp(-\mathrm{i}\phi^{(\mathrm{L})}) , \\
\boldsymbol{E}^{(\mathrm{R})} &= E_0(\boldsymbol{e}_X - \mathrm{i}\boldsymbol{e}_Y)\exp(-\mathrm{i}\phi^{(\mathrm{R})}) , \\
\boldsymbol{B}^{(\mathrm{L})} &= B_0(-\mathrm{i}\boldsymbol{e}_X + \boldsymbol{e}_Y)\exp(-\mathrm{i}\phi^{(\mathrm{L})}) , \\
\boldsymbol{B}^{(\mathrm{R})} &= B_0(\mathrm{i}\boldsymbol{e}_X + \boldsymbol{e}_Y)\exp(-\mathrm{i}\phi^{(\mathrm{R})}) ,
\end{aligned}
\tag{6}
$$

of the electromagnetic plane wave. Here E_0 and B_0 are scalar amplitudes, and $\boldsymbol{e}_X$ and $\boldsymbol{e}_Y$ are unit vectors in the X and Y axes of the frame (X, Y, Z). The phases $\phi^{(\mathrm{L})}$ and $\phi^{(\mathrm{R})}$ are different for left and right electromagnetic plane waves:

$$
\begin{aligned}
\phi^{(\mathrm{L})} &= \omega t - \boldsymbol{\kappa}^{(\mathrm{L})} \cdot \boldsymbol{r} , \\
\phi^{(\mathrm{R})} &= \omega t - \boldsymbol{\kappa}^{(\mathrm{R})} \cdot \boldsymbol{r} ,
\end{aligned}
\tag{7}
$$

where ω is the angular frequency of the wave in radians per second at an instant t (s); $\boldsymbol{\kappa}^{(L)}$ and $\boldsymbol{\kappa}^{(R)}$ are the left and right wave vectors in inverse metres at a position $\boldsymbol{r}$ in metres.

For the FMD simulation we approximate the phases by

$$\phi = \phi^{(L)} = \phi^{(R)} = \omega t \,, \tag{8}$$

which is valid at far infrared and infrared frequencies.

With these definitions therefore we can write out the torques as follows, (1) for the ORD polarisability, (2) for the CD polarisability.

(1) *Torque with frequency doubling due to the ORD tensor*

$$\begin{aligned}
T_1^{(L)(R)} &= \{({}^m\gamma^e_{12} - {}^m\gamma^e_{21})[(e_{1X}e_{3Y} + e_{3X}e_{1Y})\sin 2\phi \pm (e_{3X}e_{1X} - e_{3Y}e_{1Y})\cos 2\phi] \\
&\quad + ({}^m\gamma^e_{23} - {}^m\gamma^e_{32})[2e_{1X}e_{1Y}\sin 2\phi \pm (e^2_{1X} - e^2_{1Y})\cos 2\phi] \\
&\quad + ({}^m\gamma^e_{31} - {}^m\gamma^e_{13})[(e_{1X}e_{2Y} + e_{2X}e_{1Y})\sin 2\phi \pm (e_{1X}e_{2X} - e_{1Y}e_{2Y})\cos 2\phi]\} E_0B_0 \,, \\
T_2^{(L)(R)} &= \{({}^m\gamma^e_{23} - {}^m\gamma^e_{32})[(e_{2X}e_{1Y} + e_{1X}e_{2Y})\sin 2\phi \pm (e_{1X}e_{2X} - e_{1Y}e_{2Y})\cos 2\phi] \\
&\quad + ({}^m\gamma^e_{31} - {}^m\gamma^e_{13})[2e_{2X}e_{2Y}\sin 2\phi \pm (e^2_{2X} - e^2_{2Y})\cos 2\phi] \\
&\quad + ({}^m\gamma^e_{12} - {}^m\gamma^e_{21})[(e_{2X}e_{3Y} + e_{3X}e_{2Y})\sin 2\phi \pm (e_{2X}e_{3X} - e_{2Y}e_{3Y})\cos 2\phi]\} E_0B_0 \,, \\
T_3^{(L)(R)} &= \{({}^m\gamma^e_{31} - {}^m\gamma^e_{13})[(e_{3X}e_{2Y} + e_{2X}e_{3Y})\sin 2\phi \pm (e_{2X}e_{3X} - e_{2Y}e_{3Y})\cos 2\phi] \\
&\quad + ({}^m\gamma^e_{12} - {}^m\gamma^e_{21})[2e_{3X}e_{3Y}\sin 2\phi \pm (e^2_{3X} - e^2_{3Y})\cos 2\phi] \\
&\quad + ({}^m\gamma^e_{23} - {}^m\gamma^e_{32})[(e_{3X}e_{1Y} + e_{1X}e_{3Y})\sin 2\phi \pm (e_{3X}e_{1X} - e_{3Y}e_{1Y})\cos 2\phi]\} E_0B_0 \,.
\end{aligned} \tag{9}$$

(2) *Torque with frequency doubling due to the CD tensor*

$$\begin{aligned}
T_1^{(L)(R)} &= \{({}^m\gamma'^e_{12} - {}^m\gamma'^e_{21})[-(e_{1X}e_{3Y} + e_{3X}e_{1Y})\cos 2\phi \pm (e_{3X}e_{1X} - e_{3Y}e_{1Y})\sin 2\phi] \\
&\quad + ({}^m\gamma'^e_{23} - {}^m\gamma'^e_{32})[-2e_{1X}e_{1Y}\cos 2\phi \pm (e^2_{1X} - e^2_{1Y})\sin 2\phi] \\
&\quad + ({}^m\gamma'^e_{31} - {}^m\gamma'^e_{13})[-(e_{1X}e_{2Y} + e_{2X}e_{1Y})\cos 2\phi \pm (e_{1X}e_{2X} - e_{1Y}e_{2Y})\sin 2\phi]\} E_0B_0 \,, \\
T_3^{(L)(R)} &= \{({}^m\gamma'^e_{23} - {}^m\gamma'^e_{32})[-(e_{2X}e_{1Y} + e_{1X}e_{2Y})\cos 2\phi \pm (e_{1X}e_{2X} - e_{1Y}e_{2Y})\sin 2\phi] \\
&\quad + ({}^m\gamma'^e_{31} - {}^m\gamma'^e_{13})[-2e_{2X}e_{2Y}\cos 2\phi \pm (e^2_{2X} - e^2_{2y})\sin 2\phi] \\
&\quad + ({}^m\gamma'^e_{12} - {}^m\gamma'^e_{21})[-(e_{2X}e_{3Y} + e_{3X}e_{2Y})\cos 2\phi \pm (e_{2X}e_{3X} - e_{2Y}e_{3Y})\sin 2\phi]\} E_0B_0 \,, \\
T_2^{(L)(R)} &= \{({}^m\gamma'^e_{31} - {}^m\gamma'^e_{13})[-(e_{3X}e_{2Y} + e_{2X}e_{3Y})\cos 2\phi \pm (e_{2X}e_{3X} - e_{2Y}e_{3Y})\sin 2\phi] \\
&\quad + ({}^m\gamma'^e_{12} - {}^m\gamma'^e_{21})[-2e_{3X}e_{3Y}\cos 2\phi \pm (e^2_{3X} - e^2_{3Y})\sin 2\phi] \\
&\quad + ({}^m\gamma'^e_{23} - {}^m\gamma'^e_{32})[-(e_{3X}e_{1Y} + e_{1X}e_{3Y})\cos 2\phi \pm (e_{3X}e_{1X} - e_{3Y}e_{1Y})\sin 2\phi]\} E_0B_0 \,.
\end{aligned} \tag{10}$$

Note that these are written in frame (1, 2, 3) and must be transformed back into frame (X, Y, Z) through the rotation matrix

$$\begin{bmatrix} T_X \\ T_Y \\ T_Z \end{bmatrix} = \begin{bmatrix} e_{1X} & e_{2X} & e_{3X} \\ e_{1Y} & e_{2Y} & e_{3Y} \\ e_{1Z} & e_{2Z} & e_{3Z} \end{bmatrix} \begin{bmatrix} T_1 \\ T_2 \\ T_3 \end{bmatrix}, \tag{11}$$

which is coded into the FMD algorithm at the appropriate point in the forces loop [1–6]. In this notation, e_{1X} for example means the X laboratory frame component of the unit vector $\boldsymbol{e}_1$ defined in the axis 1 of frame (1, 2, 3), the frame of the principal molecular moments of inertia of (S)-CHBrClF.

We narrow consideration at this point to the torque of type (1), using the ORD tensor. In C_1 molecular point group symmetry it has nine independent scalar elements [18, 19]. In the absence of ab initio or experimental data these were coded in as in ref. [5], i.e.

$$^{m}\gamma^{e}_{12} : {}^{m}\gamma^{e}_{13} : {}^{m}\gamma^{e}_{21} : {}^{m}\gamma^{e}_{23} : {}^{m}\gamma^{e}_{31} : {}^{m}\gamma^{e}_{32} = 4:5:6:7:8:9 , \tag{12}$$

and the torque of type (1) used as follows to generate second order rise transients (RTs) and time correlation functions (CFs) in the statistically stationary state in the presence of the torque.

3. Summary of FMD methods

The methods used to provide numerical evidence for BAFD are similar to those used in ref. [5], so that only a brief summary of differences is needed here. The key difference, as in section 2, is the inclusion of frequency doubling, which is represented in the torque eq. (9) by the cosine and sine terms of twice the phase. The analytical expressions for the torques (9) and (10) are also distinctly different from that in ref. [5] for the torque with zero phase.

The torque (9) of this paper was coded into the algorithm TETRA [1–6] at the appropriate point in the forces loop, and the FMD method applied with a time step of 5.0 fs for 108 molecules of (S)-CHBrClF interacting with a Lennard-Jones site potential described fully in ref. [5]. For 2000 time steps following the application of the torque, transient orientational averages of the following type were computed

$$\langle e^n_{1i} \rangle ; \quad \langle e^n_{2i} \rangle ; \quad \langle e^n_{3i} \rangle ; \quad i = X, Y, Z , \tag{13}$$

where n is a positive definite integer, and where $\langle\ \rangle$ denotes a simple average at each time step over the 108 molecules. The temperature rescaling routine used to control the pressure and temperature during this interval is described fully in refs. [5] and [6], and the code is available in full in the literature [20]. Video animations of the process are also available [11] on cassettes for the interested reader.

The transients reach a saturation level [1–6] in those cases where a Langevin or Langevin–Kielich function [1–6] is definable. In BADF this saturation level was assumed to have been reached after 2000 time steps (see following section), because another key difference between conventional ORD (ref. [5]) and BAFD is that the Langevin–Kielich function exists for ORD but does not exist for BAFD. In the saturation condition time correlation functions were computed of the molecular net angular momentum (J), molecular orientation, defined through vector $\boldsymbol{e}_1$, and molecular rotational velocity ($\dot{\boldsymbol{e}}_1$, the time derivative of $\boldsymbol{e}_1$). These correlation functions are, respectively:

$$C_{1ij} = \frac{\langle J_i(t) J_j(0) \rangle}{\langle J_i^2 \rangle^{1/2} \langle J_j^2 \rangle^{1/2}} , \tag{14}$$

$$C_{2ij} = \frac{\langle e_{1i}(t)e_{1j}(0)\rangle}{\langle e_{1i}^2\rangle^{1/2}\langle e_{1j}^2\rangle^{1/2}}\ , \tag{15}$$

$$C_{3ij} = \frac{\langle \dot{e}_{1i}(t)\dot{e}_{1j}(0)\rangle}{\langle \dot{e}_{1i}^2\rangle^{1/2}\langle \dot{e}_{1j}^2\rangle^{1/2}}\ . \tag{16}$$

Here i and j denote laboratory frame indices and can be any combination of X, Y and Z. For auto-correlation functions, $i = j$; for cross-correlation functions, i and j are different indices. These correlation functions were evaluated at two different angular frequencies $\omega = 6$ MHz, and $\omega = 60.0$ THz using running time averaging over 6000 time steps.

All production runs were made on the IBM 3090-6S computer of ETH, and estimates of the noise levels in the simulations were obtained from two contiguous segments of 6000 time steps each. The noise level rarely exceeded about 5% in the time correlation functions. In the rise transients, the noise level was higher, because simple averaging was utilised rather than running time averaging as in the correlation functions. The rise transient noise level is actually observable in fig. 1 at 60 THz.

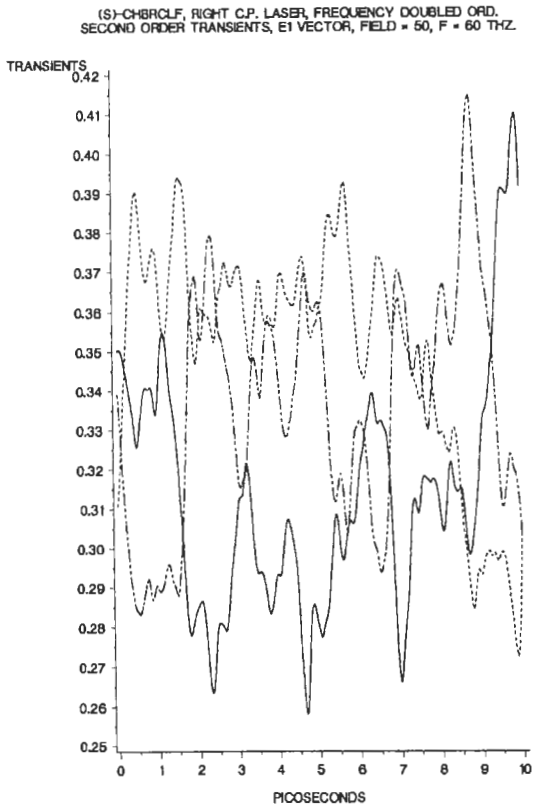

Fig. 1. Example of second order transients $\langle e_{1i}^2\rangle$ under the torque (9). No anisotropy develops.——X component;– – –Y component;– · · – · · Z component of the laboratory frame (X, Y, Z).

4. Results: bi-axial Rosenfeld anisotropy with torque frequency dependence

At both frequencies the transient orientational averages (13) were observed to fluctuate around their initial value at the instant ($t = 0$) of torque application. An example is given in fig. 1 for the second order transients $\langle e_i^2 \rangle$. This pattern was observable for $n = 1$ to 4 for all three unit vectors $\boldsymbol{e}_1$, $\boldsymbol{e}_2$, and $\boldsymbol{e}_3$. This means that the torque (9) does not generate Langevin–Kielich functions [1] which are defined [1–6] by a plot of the saturation level of an appropriate orientational rise transient against the energy per molecule transferred by the electromagnetic radiation through the torque. This is in contrast to the results of ref. [5] for ORD and CD, and the accompanying bi-axial birefringence, where Langevin–Kielich functions from analytical theory and FMD simulation were found to agree closely. In this work also, agreement has been achieved between FMD and analytical theory, in that the latter also predicts a vanishing Langevin–Kielich function for BAFD because the energy of interaction equivalent to the torque (9) vanishes when averaged over time.

Despite the absence of a Langevin–Kielich function, however, figs. 2–7 show clearly the presence of an anisotropy in the molecular dynamics due to the torque (9), an anisotropy which manifests itself through a different time evolution of the correlation functions (14)–(16). It is this anisotropy that we cite as evidence for BAFD, and the latter has been obeserved to occur at both frequencies studied in this work. The discussion presents a qualitative argument for the link between BAFD and BBFD, and suggests an experimental configuration for the observation of BBFD.

The results in figs. 2–7 were unaffected within the noise by switching the torque (9) from left to right at 60.0 THz. However at 6 MHz a small difference was detected (figs. 8–10).

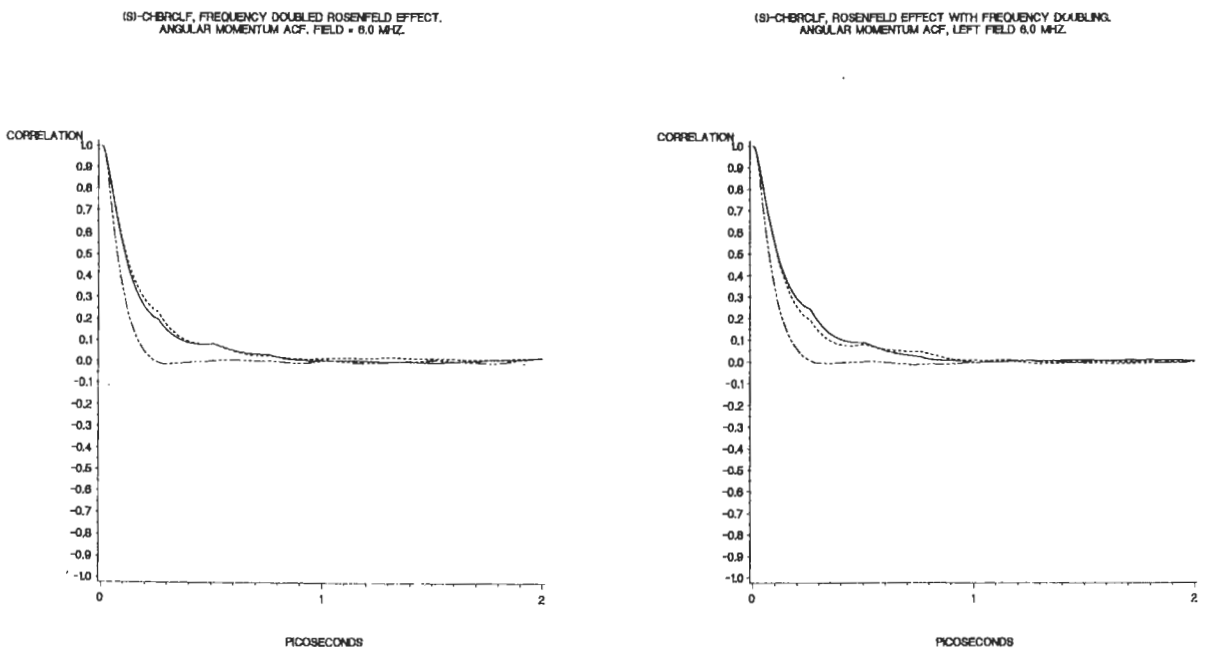

Fig. 2. Angular momentum autocorrelation functions, $\omega_p = 6$ MHz; (a) right (b) left circularly polarised radiation. X, Y, and Z components as in fig. (1).

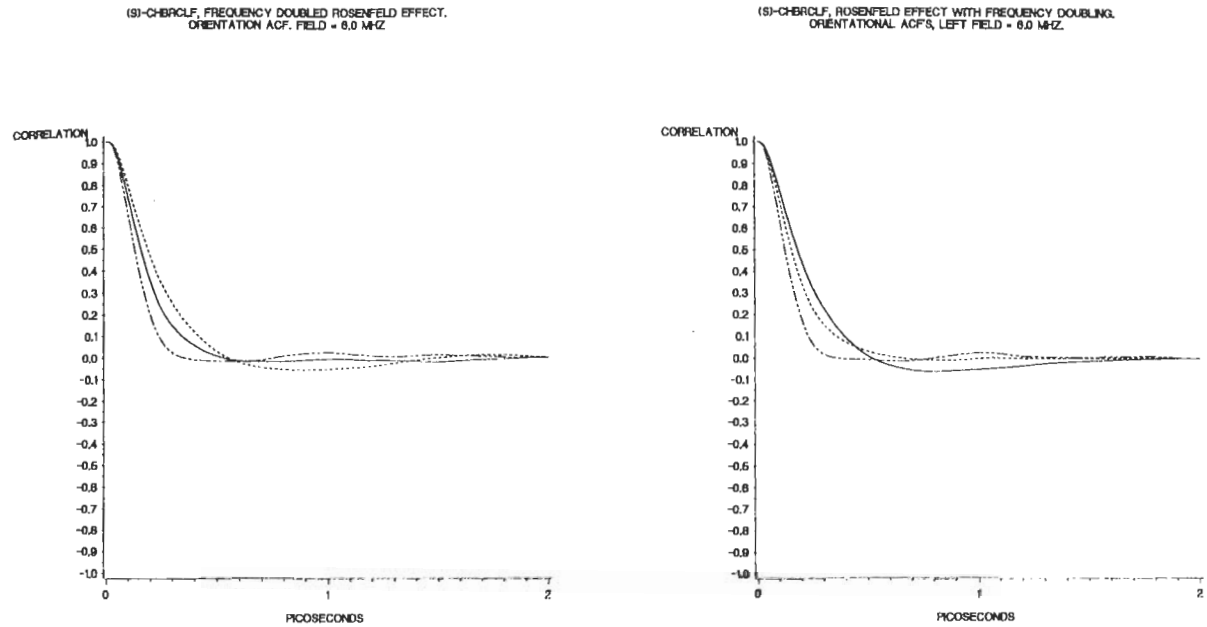

Fig. 3. As for fig. 2, orientational ACFs.

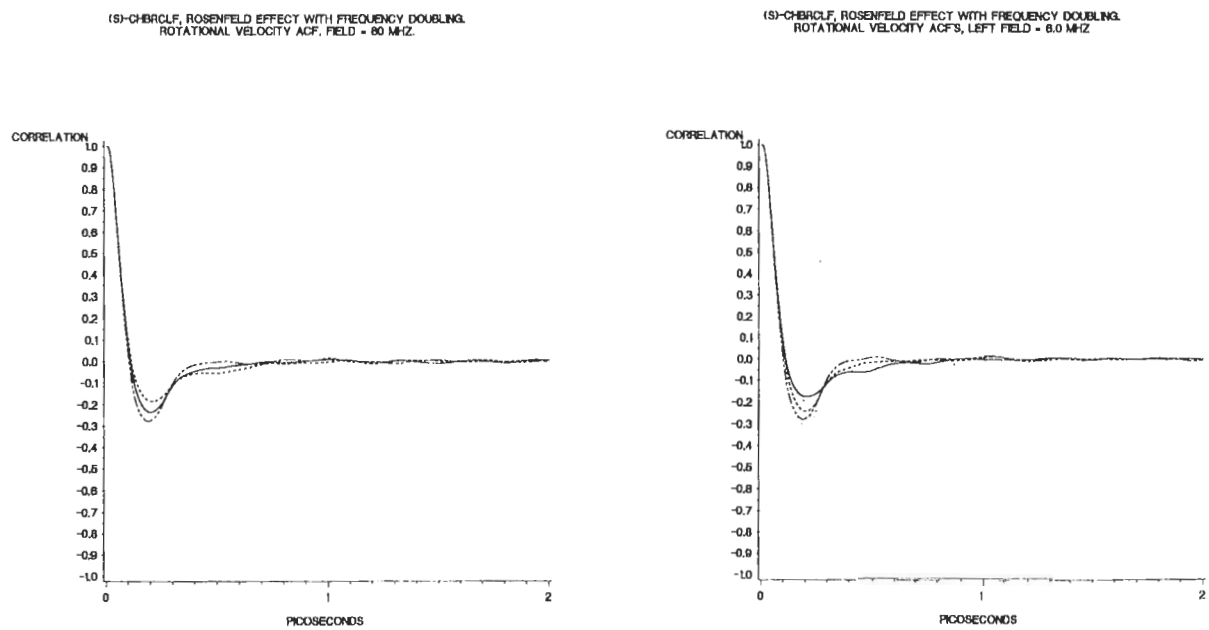

Fig. 4. As for fig. 2, rotational velocity ACFs.

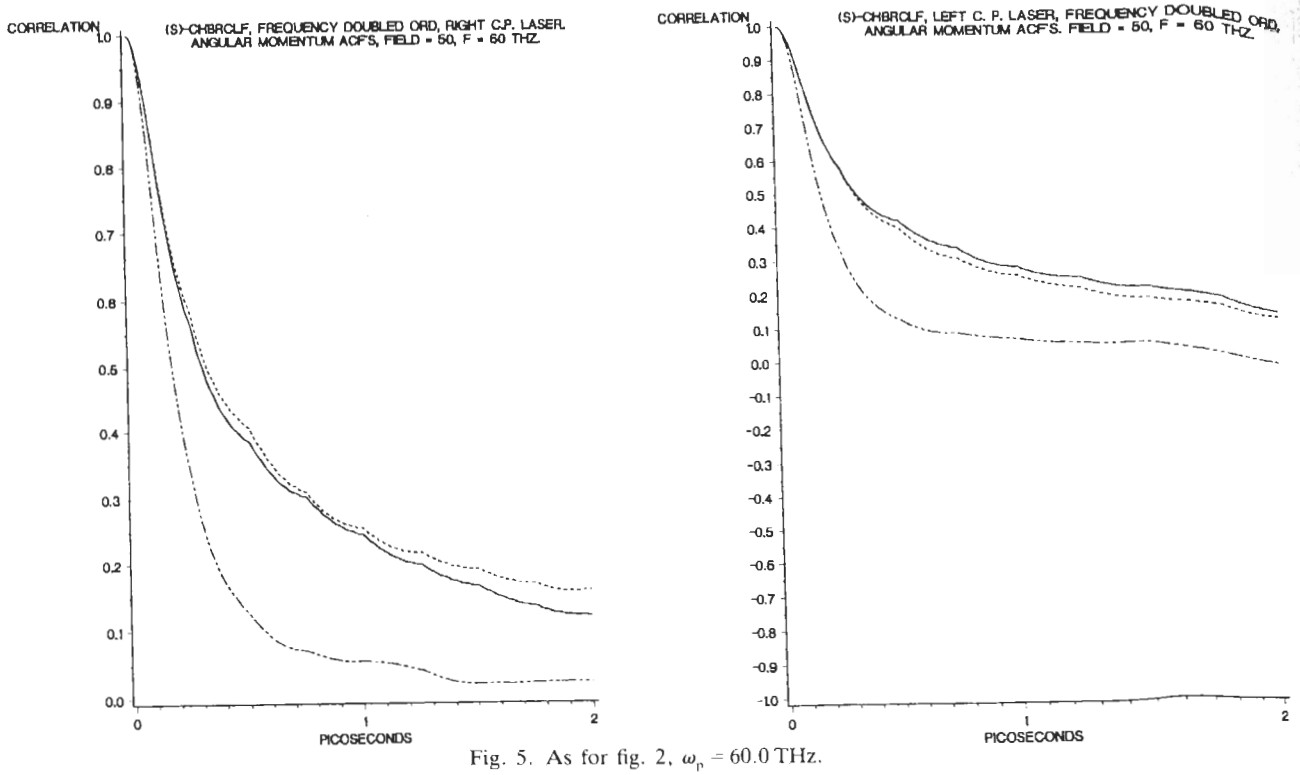

Fig. 5. As for fig. 2, $\omega_p = 60.0$ THz.

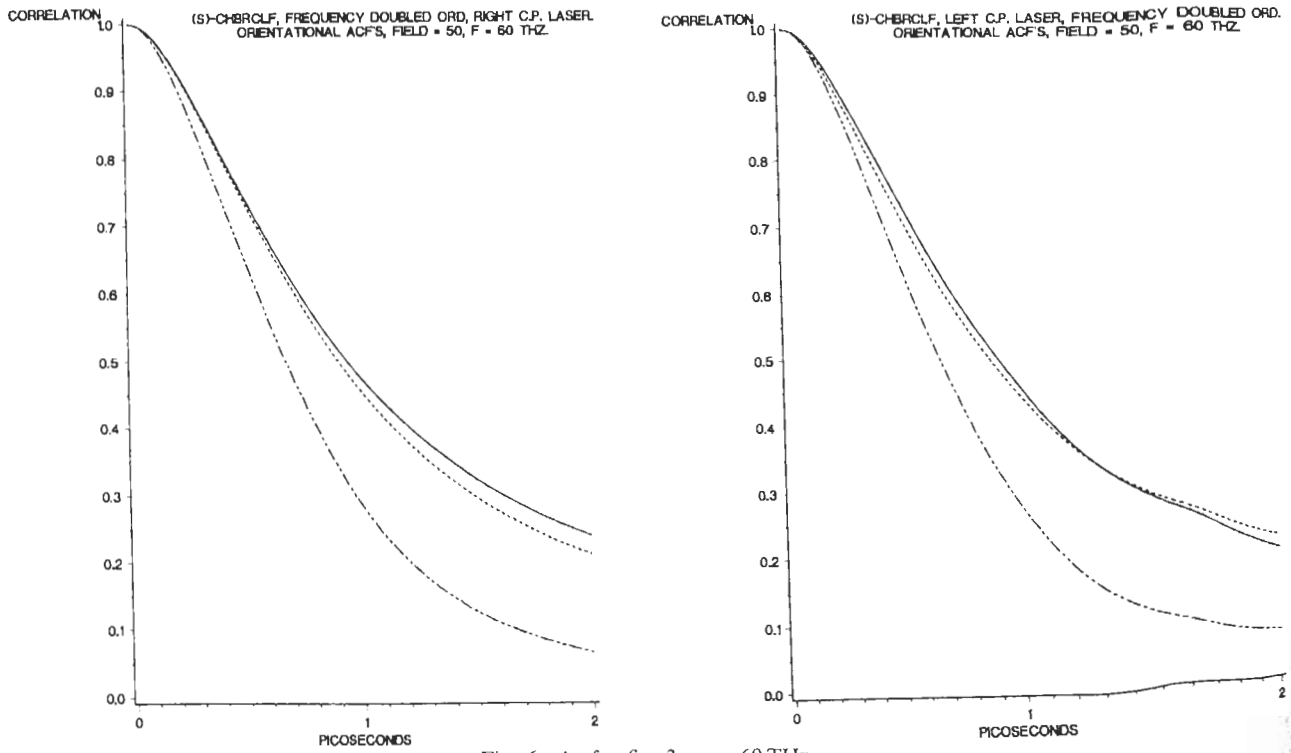

Fig. 6. As for fig. 3, $\omega_p = 60$ THz.

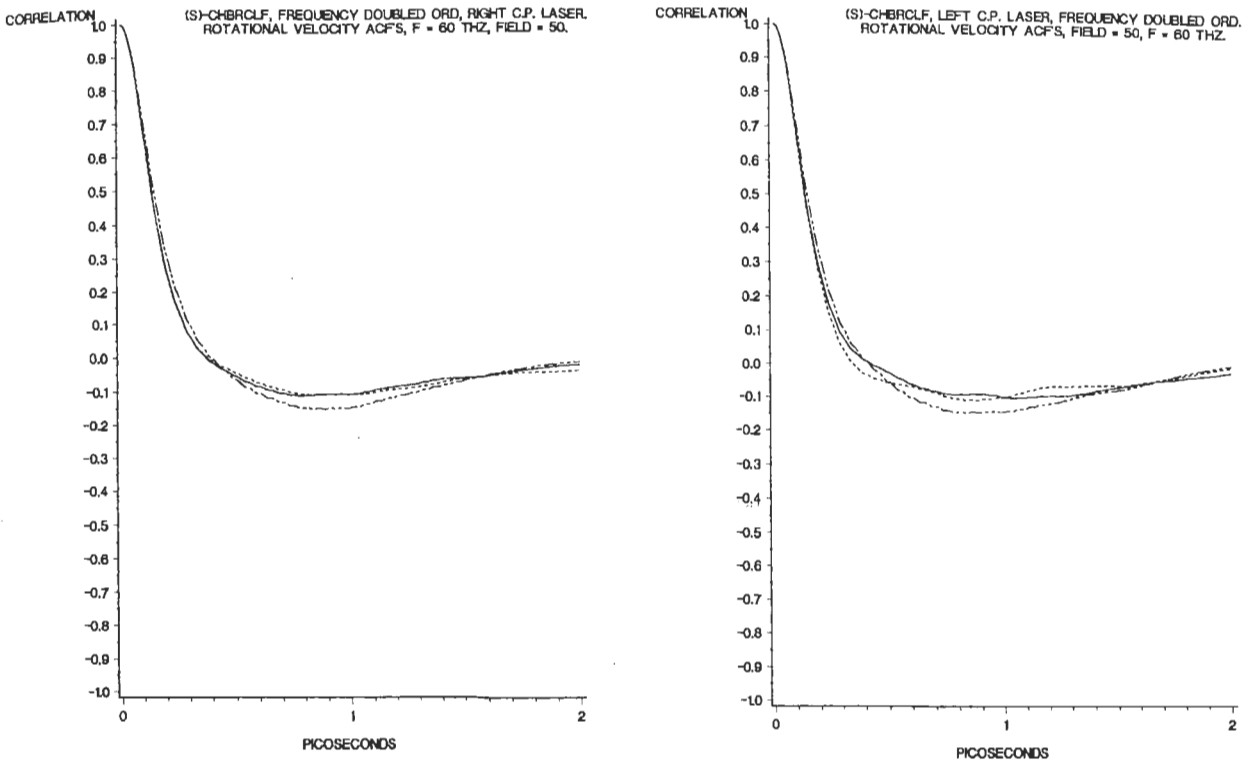

Fig. 7. As for fig. 4, $\omega_p = 60$ THz.

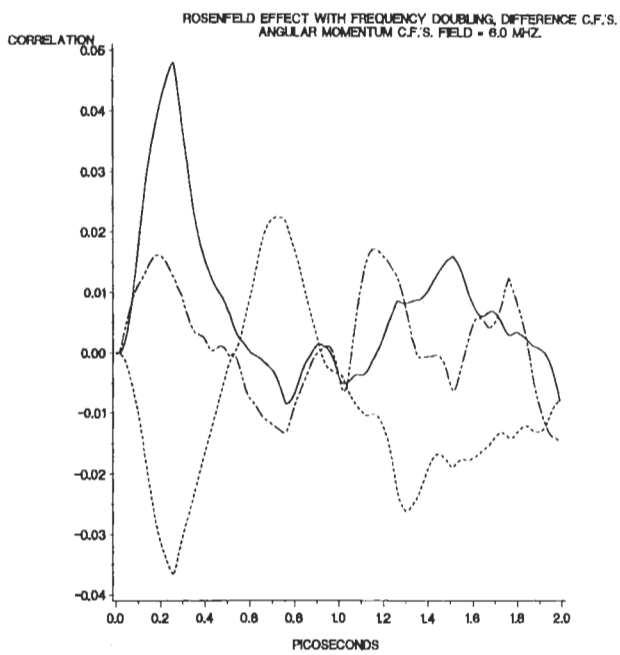

Fig. 8. Difference correlation functions of angular momentum, left minus right, at $\omega_p = 6$ MHz.

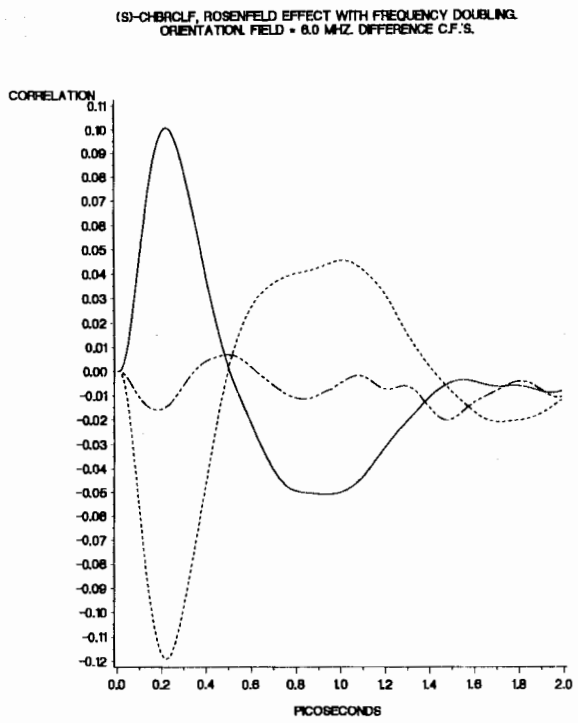

Fig. 9. Difference correlation functions of orientation, left minus right.

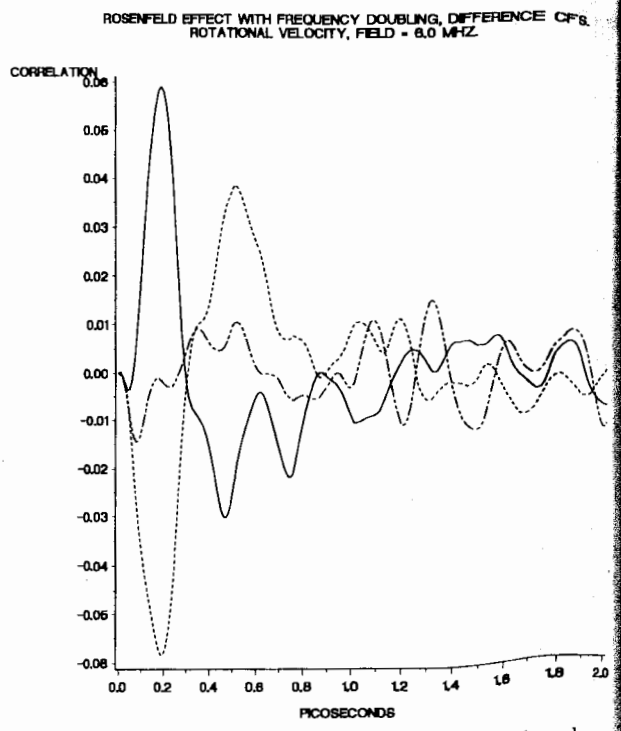

Fig. 10. Difference correlation functions of rotational velocity, left minus right.

5. Discussion

Numerical evidence has been cited for BAFD through the different evolution of time correlation functions, figs. 2–7, which in absence of the torque (9) evolve in time identically (because the liquid sample is isotropic [19]). The key implication is that the sample under the torque (9) is no longer isotropic, and therefore we have an anisotropy which is bi-axial because the time correlation function component $i = j = Z$ is different from the other orthogonal counterparts in frame (X, Y, Z). If the sample is anisotropic its spectral properties measured in axis Z (the propagation axis for torque (9)) and the orthogonal axes are different. It is well known, for example, that the Fourier transform of the orientational time correlation function is related to dielectric complex permittivity [21] and we draw the immediate conclusion from figs. 3 and 6 that dielectric loss and dielectric permittivity are different in orthogonal axes if measured under the influence of the torque (9) even though there are no Langevin–Kielich functions. This is not an easy thing to see without FMD simulation, and we have been unable to find any trace in the analytical literature of bi-axial phenomena due to the Rosenfeld tensor, either of the type described in this paper or in ref. [5]. Clearly, this shows the predictive ability of FMD in non-linear optics in general. The complex dielectric permittivity and complex refractive index are related simply by

$$\hat{\epsilon} = \hat{n}^2 , \tag{17}$$

i.e. the square of the complex refractive index is the complex permittivity. It follows that the torque (9)

produces birefringence, i.e. BBFD. In future work we hope to be able to solve the Maxwell equations for BBFD and for the novel bi-axial phenomena of ref. [5] in order to give quantitative estimates of the bi-axial birefringence in terms of the relevant Rosenfeld tensors.

In order to observe BBFD experimentally, the following simple configuration is suggested. No doubt there are more sophisticated variations which might suggest themselves to interested experimentalists.

We note from the FMD results of section 4 that BBFD is independent, at 60 THz, of the left or right circular polarity of the electromagnetic radiation passing through the ensemble in the Z axis. Furthermore, the torque (9) is quite different in nature when we use plane polarised radiation. The latter has equal amounts of right and left circularly polarised radiation, so that the cosine terms in eq. (9) vanish, leaving only the sine terms. (The cosine terms change sign for fully right and fully left circularly polarised plane waves, but the sine terms do not.) It follows that the refractive index measured in axis Z by the incoming plane wave will be measurably different in theory when the radiation is circularly polarised as opposed to linearly (or incoherently) polarised. This is the basis for a very simple experimental measurement, therefore, of the effect of the torque (9) and of the new effects presented in ref. [5]. In this configuration, the refractive index in axis Z should be the same, furthermore, for right and left circularly polarised radiation. To observe frequency dependent effects specifically, and in isolation of those of ref. [5] a pump probe system must probably be used, in which the pump laser tuned to frequency ω_p induces birefringence which is measured by the probe laser [22]. In BBFD and in other cases where frequency dependence has been studied by FMD [1–6] we note that the dependence is an intrinsic property of the non-linear electromagnetic development, and derives from products such as $E_i B_j$ whose phase doubles, thus generating the "second harmonic" cosine and sine terms in eq. (9).

It may be possible experimentally to use the fact that BBFD exists in linearly polarised radiation through the sine terms of eq. (9), but vanishes in linearly polarised radiation in the effect of ref. [5], the implication being that any residual birefringence observable with linearly polarised plane wave must be due to BBFD.

The frequency dependent torque considered in this paper probably does not give any measurable reorientational effect at visible frequencies of the pump laser, because the molecules of the ensemble may not be able to follow the applied electromagnetic field, and in consequence there is probably no change in the equilibrium refrative index for pump lasers at these frequencies. However, for a low frequency pump laser (figs. 8–10) we have

$$\omega_p \tau = 1 \,, \tag{18}$$

where τ is a characteristic relaxation time of the molecule, and the effect can probably be observed as a change of the refractive index measured by a probe beam at the frequency ω. The value of the refractive index changes at the frequency 2ω. From a solution of the Maxwell equations, we have found that the following ensemble averages contribute to the refractive index $n_{\pm}(\omega)$:

$$\begin{aligned} &\langle {}^{e}\beta^{e}_{XX}\rangle + \langle {}^{e}\beta^{e}_{YY}\rangle \,, \quad \langle {}^{e}\beta^{e}_{XY}\rangle - \langle {}^{e}\beta^{e}_{YX}\rangle \,, \\ &\langle {}^{m}\gamma^{e}_{XY}\rangle - \langle {}^{m}\gamma^{e}_{YX}\rangle \,, \quad \langle {}^{m}\gamma^{e}_{XX}\rangle + \langle {}^{m}\gamma^{e}_{YY}\rangle \,. \end{aligned} \tag{19}$$

The statistical averaging in all terms of the above must be done with the statistical distribution function $\gamma(\Omega, \boldsymbol{E}, \beta)$, which should be obtained from the kinetic diffusion equation [23]. The expression we have obtained for the change in refractive index due to our frequency dependent torque is

$$n_{\pm} = 1 + \frac{N}{4\epsilon_0}\left[\langle {}^{e}\alpha^{e}_{XX}\rangle + \langle {}^{e}\alpha^{e}_{YY}\rangle \mp i(\langle {}^{e}\alpha^{e}_{XY}\rangle - \langle {}^{e}\alpha^{e}_{YX}\rangle) + \frac{1}{c}(\langle {}^{e}\alpha^{m}_{XY}\rangle - \langle {}^{e}\alpha^{m}_{YX}\rangle - \langle {}^{m}\alpha^{e}_{XY}\rangle + \langle {}^{m}\alpha^{e}_{YX}\rangle) \pm \frac{i}{c}(\langle {}^{e}\alpha^{m}_{XX}\rangle + \langle {}^{e}\alpha^{m}_{YY}\rangle - \langle {}^{m}\alpha^{e}_{XX}\rangle - \langle {}^{m}\alpha^{e}_{YY}\rangle)\right]. \quad (20)$$

In this expression, the nonlinear terms due to nonlinear distortion of the electronic orbitals are not included. The nonlinear terms in eq. (19) all refer to orientational effects of our nonlinear torque, and it can be seen in general that the refractive index is different for right (+) and left (−) circular polarisation. It is significant that this difference is observed through correlation functions in the computer simulation when the pump laser frequency is low (6 MHz pump laser), where the molecules can follow the field, but not at high frequencies (60 THz pump laser). The analytical expression (19) for the refractive index was derived from a solution of the Maxwell equations for a probe beam with angular frequency ω and a pump beam with angular frequency ω_p.

Acknowledgements

Professor Dr. Georges Wagnière is thanked for invitations to both authors to the University of Zurich at Irchel. MWE thanks the Swiss NSF for funding this project, and ETH, Zurich for a major grant of computer time on the IBM 3090-6S supercomputer. Dr. L.J. Evans is thanked for invaluable help with the laser plotting facilities of the Irchel mainframe.

References

[1] M.W. Evans, S. Woźniak and G. Wagnière, Physica B 173 (1991) 357.
[2] M.W. Evans, S. Woźniak and G. Wagnière, Physica B 175 (1991) 412.
[3] M.W. Evans, S. Woźniak and G. Wagnière, Physica B 176 (1992) 33.
[4] M.W. Evans, Chem. Phys. 157 (1991) 1.
[5] M.W. Evans, S. Woźniak and G. Wagnière, Phys. Rev. Lett., submitted; Physica B, in press.
[6] M.W. Evans, Z. Phys. B 85 (1991) 135.
[7] J.B. Hasted, Aqueous Dielectrics (Chapman and Hall, London, 1973).
[8] N.B. Delmo and V.P. Krainov, Fundamentals of Non-Linear Optics (Wiley, New York, 1988).
[9] A.A. Abrikosov, L.P. Gorkov and I.E. Dzyaloshinski, Methods of Quantum Field Theory in Statistical Physics (Dover, New York, 1975).
[10] M.W. Evans and C.R. Pelkie, Proc. 1990 IBM Supercomputer Competition and Conference, in press.
[11] M.W. Evans and C.R. Pelkie, J. Opt. Soc. America B, in press; half hour animation video judged best graphics back up in the natural sciences category of ref. [10].
[12] M.W. Evans, G.J. Evans, W.T. Coffey and P. Grigolini, Molecular Dynamics (Wiley Interscience, New York, 1982).
[13] J. Jortner, R.D. Levine, I. Prigogine and S.A. Rice, eds., Advances in Chemical Physics Vol. 47, Pts. 1 and 2 (Wiley Interscience, New York, 1981).
[14] C. Kalpouzos, D. McMorrow, W.T. Lotshaw and G.A. Kenney-Wallace, Chem. Phys. Lett. 150 (1988) 138.
[15] P.L. Polavarapu, P.G. Quincey and J.P. Birch, Infra-red Phys. 30 (1990) 175.
[16] S.J. Giancorsi, K.M. Spencer, T.B. Freedman and L.A. Nafie, J. Am. Chem. Soc. 111 (1989) 1913.
[17] L.D. Barron, Molecular Light Scattering and Optical Activity (Cambridge Univ. Press, Cambridge, 1982).
[18] S. Woźniak and R. Zawodny, Acta Phys. Pol. A 61 (1982) 175; Chem. Phys. 103 (1986) 303.
[19] M.W. Evans, in: Advances in Chemical Physics, Vol. 81, eds. I. Prigogine and S.A. Rice (Wiley Interscience, New York, 1992) in press.
[20] C. Brot, in: Dielectric and Related Molecular Processes, Vol. 2, M. Davies (senior reporter) (Chem. Soc. Specialist Per. Rep., London, 1975) p.1.
[21] D.C. Hanna, M.A. Yuratich and D. Cotter, in: Non-Linear Optics of Free Atoms and Molecules (Springer, New York, 1979).
[22] Y.R. Shen, The Principles of Non-Linear Optics (Wiley, New York, 1984).
[23] S. Kielich, Acta Phys. Pol. 31 (1967) 929.